1

Fluid–Structure Interaction

A short overview of some analytical models and numerical methods is proposed in this chapter as an introduction to fluid–structure interaction (FSI). The analytical models derived in what follows focus on the description of the so-called inertial effect on the one hand and of vibro-acoustic coupling on the other hand, both being investigated from various points of view in the subsequent chapters. The principles of a coupled simulation are also concisely exposed and illustrated with a few specific examples borrowed from academic researches and industrial applications, thereby highlighting the variety of possible approaches on FSI. The interactions between a vibrating structure and a stagnant fluid are described by a set of partial differential equations whose numerical solution can be obtained from finite element or boundary element discretisation, both numerical techniques being presented and studied in a detailed manner in this book.


Figure 1.1   Fluids and Solids. The interactions between mechanical systems are of various nature and intensity. Structural and fluid dynamics have long been considered in a separate manner, which holds only when the fluid flow and the structure motion are weakly coupled, that is, when their evolutions occur within different characteristic times. When it is more pronounced, FSI has to be accounted for in numerical simulations: for instance, vibrations of an elastic structure in contact with a quiescent fluid are commonly described with finite element-based techniques. *Source*: © Jean-François Sɪɢʀɪsᴛ

1.1   A Wide Variety of Problems

FSI is concerned with the coupled dynamics of structures in contact with a fluid. As sketched in Figure 1.2, the basic mechanism of fluid and structure coupling may be described as follows: the motion of the structure modifies the flow conditions at the interface with the fluid, which in turn induces a fluctuation in the pressure and/or viscous forces; the loading applied to the fluid–structure interface subsequently changes the structure motion.

A wide variety of industrial problems, ranging from civil to naval and offshore engineering, from transportation to medical applications, from power nuclear to aerospace industries, are concerned by FSI. From an engineering perspective, taking FSI into account is often of major importance since the structural response to fluid loading enters into consideration for safety, reliability or durability issues of mechanical systems – for instance, in shipbuilding, the so-called hydrodynamic impact is a rather spectacular illustration of FSI; see Figure 1.3.

FSI modelling usually assumes that both the structure and the fluid parts of a coupled system are studied within the theoretical framework of the continuum mechanics. As a consequence, their motion is governed by a set of partial differential equations associated with some appropriate boundary conditions. However, in certain circumstances, specified later when needed, it may be found advantageous to formulate the differential equations of the fluid motion into an integral form.
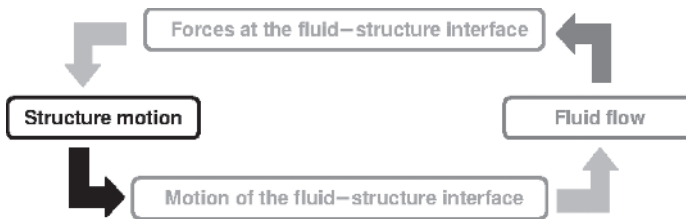
Figure 1.2   Fluid–structure interaction: coupling mechanism

Figure 1.3   Hydrodynamic impact. Among many phenomena involving fluid and structure motions in extreme conditions, *slamming* is one of the most spectacular examples of fluid–structure interaction. When sailing at high speed and/or in rough sea condition, the impact of a ship on water induces high loads on the structure: slamming is, among other cases, of primary concern when designing ships. *Source*: © A.Monot/Marine Nationale

Analytical solutions to the equations of motion can be made available for simple geometries of the solid and fluid domains, scarcely met in practice. Such particular cases are of academic interest, for instance, in order to highlight some essential features of FSI, as first considered in Section 1.2.

In most applications of engineering relevance, numerical methods are resorted to in order to produce approximate solutions. A short overview of the large variety of FSI problems in relation to the numerical methods made available to the designer to solve them is proposed in Section 1.3.

1.2   Analytical Modelling of Fluid–Structure Interactions

Beyond the definition of energy transfer from one medium to another lies a large number of situations: the *dimensional analysis*, as developed for instance by De Langre (2001), offers a general framework for the classification of various coupling phenomena. For a given problem, a set of non-dimensional numbers characterises the intensity of the coupling (whether 'strong' or 'weak'): it is usually derived from the fluid–structure mathematical model.

An illustration of some manifestations of FSI is proposed hereafter, starting from the vibrations of a spring-mass system, as represented in Figure 1.4.

Without fluid coupling, vibrations of the cylinder are accounted for by the equation of motion $m\ddot{u}(t) + ku(t) = 0$. It is a second-order ordinary differential equation, endowed with initial conditions $u(t=0) = u_o$ and $\dot{u}(t=0) = \dot{u}_o$. Using non-dimensional variables $u^* = u/R$, with R scaling displacement, and $t^* = \omega_o t$, with $\omega_o = \sqrt{\frac{k}{m}}$ scaling time, the non-dimensional equation of motion may be recast as follows:

$$\ddot{u}^*(t^*) + u^*(t^*) = 0 \qquad u^*(t^* = 0) = u_o^* \qquad \dot{u}^*(t = 0) = \dot{u}_o^*$$

As made conspicuous in the following subsections, analytical solutions to the fluid flow equations are conveniently derived using the Laplace transform.[1] In order to enable a

---

[1] It is recalled that when it exists, the Laplace transform of function $\psi(t)$ (denoted here $\hat{\psi}(s) = \mathcal{L}(\psi(t))$ with s the Laplace variable), and its inverse, are defined by the integrals:

$$\hat{\psi}(s) = \int_0^\infty \psi(t) \exp\,(-st)dt$$

$$\psi(t) = \mathcal{L}^{-1}(\hat{\psi}(s)) = \frac{1}{2i\pi} \int_{\sigma-i\infty}^{\sigma+i\infty} \hat{\psi}(s) \exp\,(+st)ds$$

σ is such that the integral converges (which is ensured for any σ greater than the real value of any singularity of $\hat{\psi}(s)$) and if $|\hat{\psi}(s)| = o(|s|^2)$ for $|s| \to \infty$. As illustrated in what follows, the Laplace transform is well suited for the description of time-dependent problems with initial conditions. The elementary properties of the Laplace transform, such as recalled below, make it useful for solving partial differential equations.

- The Laplace transform of a function derivative is $\mathcal{L}(\psi'(t)) = s\mathcal{L}(\psi(t)) - \psi(0)$;
- The Laplace transform of a Dirac function is $\mathcal{L}(\delta(t)) = 1$, $\forall s$;
- The Laplace transform of a function product is $\mathcal{L}(\psi_a * \psi_b(t)) = \mathcal{L}(\psi_a(t))\mathcal{L}(\psi_b(t))$, where the convolution product of ψ_a and ψ_b is defined by:

$$\psi_a * \psi_b(t) = \int_{-\infty}^{+\infty} \psi_a(t - \tau)\psi_b(\tau)d\tau$$

when the integral exists. It is recalled that a function remains unchanged when convoluted with the Dirac function: $\psi * \delta(t) = \psi(t)$.
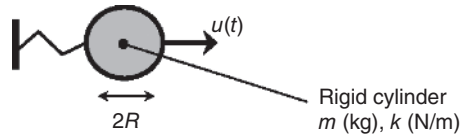
Figure 1.4   Spring-mass system. Computer simulation of mechanical systems can handle numerical models of increasing complexity. Analytical models still prove useful to understand some 'elementary' physics and to validate numerical methods

comparison with the non-coupled case, the Laplace transform of the former equation is written as follows:

$$\hat{\ddot{u}}^*(s^*) + \hat{u}^*(s^*) = 0$$

with the non-dimensional Laplace variable $s^* = \omega_o s$.

When the cylinder is coupled to a fluid initially at rest, various flow models may be considered, under the assumption that the motions of the solid are small regarded to the size of the fluid domain. Small perturbations of the pressure and/or velocity fields are considered – such assumptions will be clarified in Chapter 3. For the sake of simplicity, the equations of the fluid flow are taken for granted in what follows.

1.2.1   Potential Flow. Inertial Coupling

As depicted in Figure 1.5, the vibrations of the cylinder coupled to an inviscid and incompressible fluid are considered, assuming small amplitude perturbation of the flow. The equation of motion is $m\ddot{u} + ku = \phi$, where ϕ stands for the force exerted by the fluid. The latter is calculated as follows:

$$\phi = -\int_0^{2\pi} p(R, \theta, t) \cos \theta R \, d\theta \tag{1.1}$$

where p stands for the pressure fluctuation in the fluid.
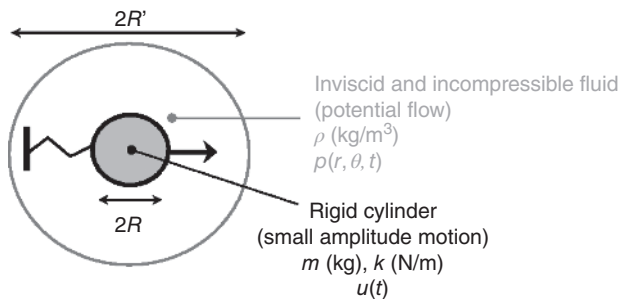
Figure 1.5   Cylinder coupled to an incompressible fluid in annular confinement (potential flow model)

Under potential flow assumptions, the fluctuation of the pressure field in the fluid is described by the Laplace equation, stated in the cylindrical coordinate system as follows:

$$\frac{\partial^2 p}{\partial r^2} + \frac{1}{r}\frac{\partial p}{\partial r} + \frac{1}{r^2}\frac{\partial^2 p}{\partial \theta^2} = 0$$

The coupling of the fluid with the moving inner wall and the fixed outer wall are expressed by the following boundary conditions:

$$\left.\frac{\partial p}{\partial r}\right|_{r=R} = -\rho \ddot{u}(t)\cos\theta \qquad \left.\frac{\partial p}{\partial r}\right|_{r=R'} = 0$$

According to Fritz (1972), the pressure field is found to be

$$p(r,\theta,t) = -\frac{\rho}{1-\alpha^2}\left(r + \frac{\alpha^2 R^2}{r}\right)\ddot{u}(t)\cos\theta$$

with $\alpha = \frac{R'}{R}$.

The pressure is proportional to the acceleration of the structure, indicating that the perturbations of the fluid flow resulting from the vibration of the structure are instantaneously propagated throughout the fluid domain. Accordingly, the pressure force on the cylinder is also found to be proportional to its acceleration:

$$\phi(t) = -\rho\pi R^2 \frac{\alpha^2+1}{\alpha^2-1}\ddot{u}(t) = -m_a\ddot{u}(t)$$

where m_a is the so-called fluid *added mass*.

The vibrations of the cylinder are therefore governed by

$$(m + m_a)\ddot{u} + ku = 0$$

which is also stated in a non-dimensional form in the Laplace domain:

$$(1 + \mathcal{M}_a)\hat{\ddot{u}}^* + \hat{u}^* = 0 \tag{1.2}$$

$\mathcal{M}_a$ is the *mass number*, defined as the ratio of the fluid added mass and the structure mass:

$$\mathcal{M}_a = \frac{\rho\pi R^2}{m}\frac{\alpha^2+1}{\alpha^2-1}$$

In the Laplace domain, the coupling is represented by the FSI function $\hat{\mu}(s^*) = \mathcal{M}_a\delta(s^*)$, so that in the time-domain, the pressure force is proportional to the structure acceleration. FSI is of *inertial nature*, and it is quantified by $\mathcal{M}_a$, as illustrated in Figure 1.6.

The fluid added mass is a *virtual* mass which accounts for the inertial effect, and, as depicted in Figure 1.7, it is usually different from the physical mass of the fluid – in the present case, the latter is $\rho\pi R^2(\alpha^2-1)$ while the former is $m_a = \rho\pi R^2\frac{\alpha^2+1}{\alpha^2-1}$.

For a strong confinement ($\alpha \ll 1$), the added mass largely exceeds the actual mass of the fluid and tends to be 'infinite' in extreme confinements ($\alpha \to 1$). For an infinite extent of
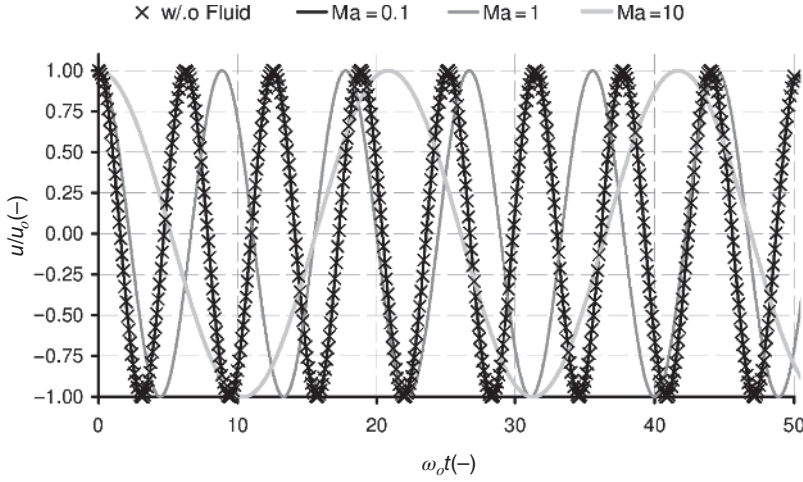
Figure 1.6   FSI effect for potential flow. The free vibrations of the cylinder without and with fluid are represented using non-dimensional values, for initial conditions $u_o^* = 1$ and $\dot{u}_o^* = 0$ and for different mass numbers. In the present case, FSI is of inertial nature: according to Equation (1.2), the cylinder vibrates with an additional inertia, so that the period of its natural vibrations increases with $\mathcal{M}_a$
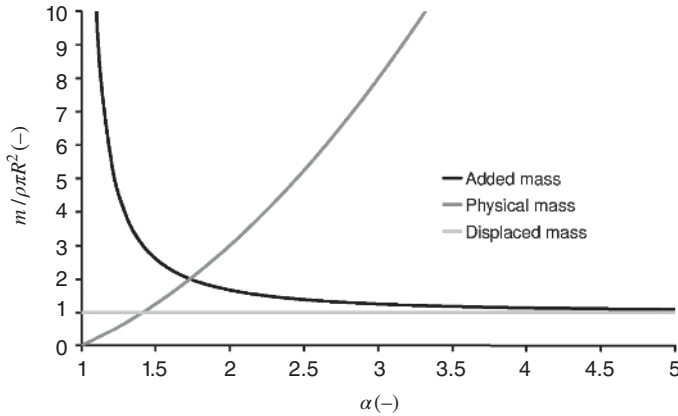
Figure 1.7   Added mass and displaced mass for a cylinder in cylindrical confinement and physical mass of fluid within the annular space

the fluid domain ($\alpha \gg 1$), it reaches a finite value $\rho \pi R^2$, which is the mass of the fluid displaced by the solid.

As the fluid is set into motion by the vibration of the structure, it gains kinetic energy. The latter is evaluated as follows:

$$\mathcal{E} = \int_R^{\alpha R} \int_0^{2\pi} \frac{1}{2} \rho (\dot{\xi}_r^2 + \dot{\xi}_\theta^2) r \, dr d\theta$$

where $\boldsymbol{\xi} = (\xi_r, \xi_\theta)$ is the fluid displacement field. For potential flows, $\boldsymbol{\xi}$ is shown to be derived from the displacement potential φ, that is, $\boldsymbol{\xi} = \nabla\varphi$. φ may be calculated from the fluid pressure according to $p = -\rho\frac{\partial^2\varphi}{\partial t^2}$, so that in the present case, the following relation is arrived at:

$$\varphi(r, \theta, t) = \frac{1}{1 - \alpha^2}\left(r + \frac{\alpha^2 R^2}{r}\right)u(t)\cos\theta$$

Hence:

$$\xi_r = \frac{\partial\varphi}{\partial r} = \frac{1}{1 - \alpha^2}\left(1 - \frac{\alpha^2 R^2}{r^2}\right)u(t)\cos\theta$$

$$\xi_\theta = \frac{1}{r}\frac{\partial\varphi}{\partial\theta} = -\frac{1}{1 - \alpha^2}\left(1 + \frac{\alpha^2 R^2}{r^2}\right)u(t)\sin\theta$$

and:

$$\mathcal{E} = \frac{1}{2}\rho\dot{u}^2\frac{\pi}{(1 - \alpha^2)}\int_R^{\alpha R}\left(\left(1 + \frac{\alpha^2 R^2}{r}\right)^2 + \left(1 - \frac{\alpha^2 R^2}{r}\right)^2\right)r\,dr$$
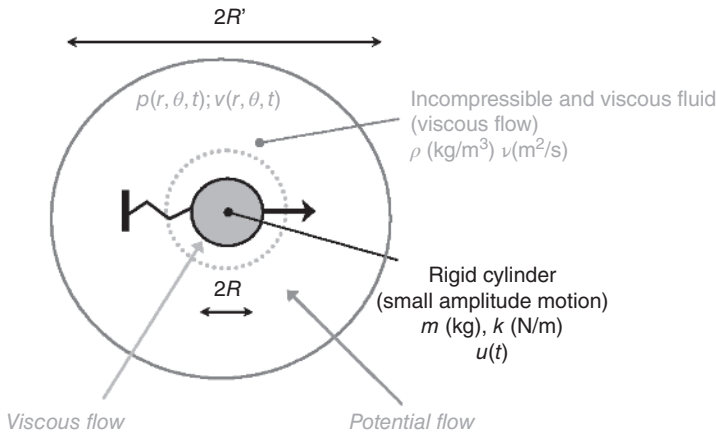
The kinetic energy in the fluid is therefore found to be:

$$\mathcal{E} = \frac{1}{2}\rho\pi R^2\frac{1 + \alpha^2}{1 - \alpha^2}\dot{u}^2 = \frac{1}{2}m_a\dot{u}^2$$

which gives a straightforward physical signification of the added mass.

1.2.2 Viscous Flow. Viscous Damping

The vibrations of a cylinder coupled to a fluid is investigated for a viscous flow, as in the configuration depicted in Figure 1.8.

Figure 1.8 Cylinder coupled with an incompressible fluid in annular confinement (viscous flow model)

The force exerted by the fluid on the cylinder is expressed as follows:

$$\phi = \int_0^{2\pi} (\cos\theta e_r + \sin\theta e_\theta)\sigma(R,\theta)e_r R \ d\theta = \int_0^{2\pi} \sigma_{rr} R\cos\theta \ d\theta + \int_0^{2\pi} \sigma_{r\theta} R\sin\theta \ d\theta$$

where σ_{rr} and $\sigma_{r\theta}$ are the fluid stress tensor components. The latter are calculated as follows:

$$\sigma_{rr} = -p + \frac{\partial v_r}{\partial r} \qquad \sigma_{r\theta} = \frac{\rho v}{2}\left(\frac{1}{r}\frac{\partial v_r}{\partial\theta} + \frac{\partial v_\theta}{\partial r} - \frac{v_\theta}{r}\right)$$

where $p(r,\theta)$ and $\mathbf{v}(r,\theta) = (v_r(r,\theta), v_\theta(r,\theta))$ stand for the fluid pressure and velocity fields, and v denotes the fluid kinematic viscosity.

As exposed in a detailed manner in Chapter 3, a fluid flow may be described by the mass and momentum equations. In the present case, these equations are expressed as follows[2], using a cylindrical coordinate system:

$$\frac{1}{r}\frac{\partial(\rho r v_r)}{\partial r} + \frac{\partial(\rho r v_\theta)}{\partial\theta} = 0$$

and:

$$\frac{\partial v_r}{\partial t} = \frac{1}{\rho}\frac{\partial p}{\partial r} + v\left(\frac{\partial^2 v_r}{\partial r^2} + \frac{1}{r}\frac{\partial v_r}{\partial r} - \frac{v_r}{r^2} + \frac{1}{r^2}\frac{\partial^2 v_r}{\partial\theta^2} - \frac{2}{r^2}\frac{\partial v_\theta}{\partial\theta}\right)$$

$$\frac{\partial v_\theta}{\partial t} = \frac{1}{\rho r}\frac{\partial p}{\partial\theta} + v\left(\frac{\partial^2 v_\theta}{\partial r^2} + \frac{1}{r}\frac{\partial v_\theta}{\partial r} - \frac{v_\theta}{r^2} + \frac{1}{r^2}\frac{\partial^2 v_\theta}{\partial\theta^2} + \frac{2}{r^2}\frac{\partial v_\theta}{\partial\theta}\right)$$

The initial conditions of the fluid flow are represented by the following relations:

$$p(t=0) = p_o \qquad v_r(t=0) = v_r^o \qquad v_\theta(t=0) = v_\theta^o$$

while the boundary conditions, namely the coupling conditions with the moving cylinder at $r = R$ and with the fixed wall at $r = R'$, are expressed as:

$$v_r(R,\theta) = \dot{u}\cos\theta \qquad v_r(R',\theta) = 0 \qquad v_\theta(R,\theta) = \dot{u}\sin\theta \qquad v_\theta(R',\theta) = 0$$

An analytical solution to the fluid flow equations may be derived using a matched asymptotic development technique: in the vicinity of the cylinder, a pure viscous flow solution is derived, while in the remainder of the fluid domain, a potential flow solution is obtained. Matching these solutions describes the fluid flow throughout the fluid domain, as sketched in Figure 1.8. An application of this technique is proposed by Leblond *et al.* (2009) for the problem under concern here; using the Laplace transform, it can be shown that the fluid force on the cylinder is expressed as follows:

$$\hat{\phi}(s) = -\rho\pi R^2\left(\frac{\alpha^2+1}{\alpha^2-1} + \frac{4\alpha^2}{\alpha^2-1}\frac{1}{\sqrt{R^2 s/v}}\right)\hat{\ddot{u}}(s)$$

In this equation, the first term is related to the potential flow, while the second term is a viscous correction. Substituting this expression of the fluid force into the equation of motion for the

---

[2] As small amplitude motions of both the cylinder and the fluid are assumed, the convection terms are discarded in the momentum equation, see Chapter 3.

cylinder yields the following equation:

$$(1 + \mathcal{M}_a \hat{\mu}(s^*/S_t))\hat{\ddot{u}}^* + \hat{u}^* = 0 \tag{1.3}$$

The above expression is formulated in the Laplace domain using non-dimensional variables. The influence of the fluid on the cylinder motion is accounted for by the *FSI function* $\hat{\mu}(s^*/S_t)$, which is expressed here as follows:

$$\hat{\mu}(s^*/S_t) = \frac{\alpha^2 + 1}{\alpha^2 - 1} + \frac{4\alpha^2}{\alpha^2 - 1} \frac{1}{\sqrt{s^*/S_t}}$$

with:

$$S_t = \frac{\nu}{\omega_o R^2}$$

S_t is the so-called *viscosity number* or Stokes number: in terms of order of magnitude, it may be interpreted as the ratio between the propagation velocity of viscous shear waves in the fluid, which is ν/R, and the vibration velocity of the cylinder, which is $\omega_o R$.

In the Laplace domain, the influence of the fluid on the solid motion is expressed by Equation (1.3) and consequently, in the time-domain, FSI is represented by the convolution product of μ^* and $\ddot{u}^*$, so that the fluid force at time t depends on the acceleration of the cylinder at time t, and also at any time $t' < t$. There is a *history effect* which is associated with the propagation of viscous shear waves in the fluid and its relative importance in comparison to the vibration velocity of the cylinder is quantified by the viscosity number, as further illustrated in Figure 1.9.
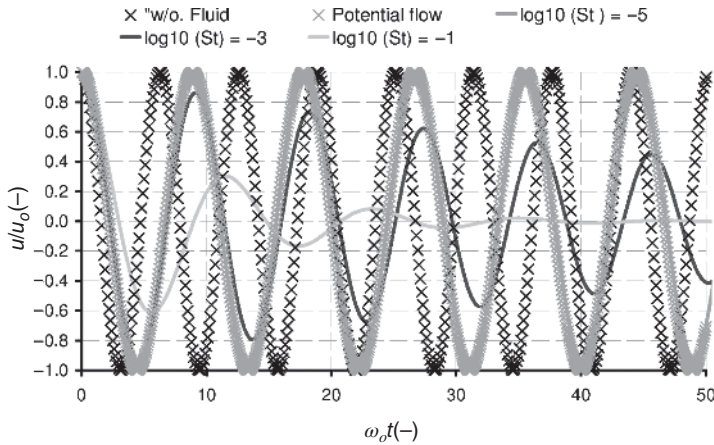
Figure 1.9   FSI effects for viscous flow. The free vibrations of the cylinder without and with fluid are represented using non-dimensional values, for initial conditions $u_o^* = 1$ and $\dot{u}_o^* = 0$ and for various viscosity numbers. For small values of S_t, FSI is mainly of inertial nature and the potential flow model suffices to account for the interactions. For larger values of S_t however, viscous effects are marked by a raise of the kinetic energy in the fluid shear layer (inertial effect is stronger than in the potential flow case), and by a dissipation of the kinetic energy which results from the friction between fluid layers

1.2.3 Compressible Flow. Radiation Damping

As represented in Figure 1.10, the vibrations of a cylinder coupled to a fluid are investigated here under the assumption of an acoustic flow in an infinite domain.

According to Equation (1.1), the fluid force ϕ is obtained by integrating the pressure around the cylinder circumference; for a compressible flow, p satisfies the acoustic wave equation, which is expressed in the present example as follows:

$$\frac{\partial^2 p}{\partial r^2} + \frac{1}{r}\frac{\partial p}{\partial r} + \frac{1}{r^2}\frac{\partial^2 p}{\partial \theta^2} - \frac{1}{c^2}\frac{\partial^2 p}{\partial t^2} = 0$$

using a cylindrical coordinate system. In the above expression, c stands for the speed of sound in the fluid.

The coupling condition with the cylinder motion at $r = R$ is stated as follows:

$$\left.\frac{\partial p}{\partial r}\right|_{r=R} = -\rho \ddot{u}(t) \cos \theta$$

A condition at infinity is also required in order for the problem to be well posed; as made conspicuous in Chapter 3, this condition states that waves travelling away from the structure are not reflected at infinity. In the Laplace domain, the former equation and boundary conditions are expressed as follows:

$$\frac{s^2}{c^2}\hat{p} - \Delta\hat{p} = 0 \qquad \left.\frac{\partial \hat{p}}{\partial r}\right|_{r=R} = -\rho \hat{\ddot{u}} \cos \theta \qquad \hat{p}|_{r\to\infty} < +\infty$$
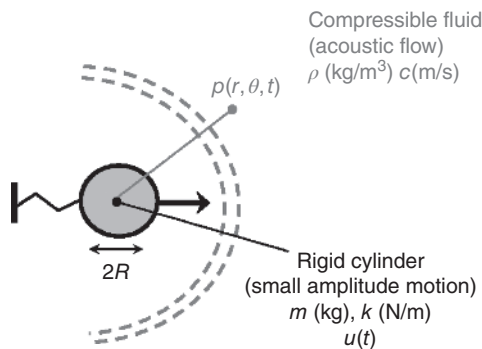
The pressure field is shown to be

$$\hat{p}(r, \theta, s) = -\rho \frac{1}{s/c}\frac{K(rs/c)}{K'(Rs/c)}\hat{u}(s)\cos\theta$$
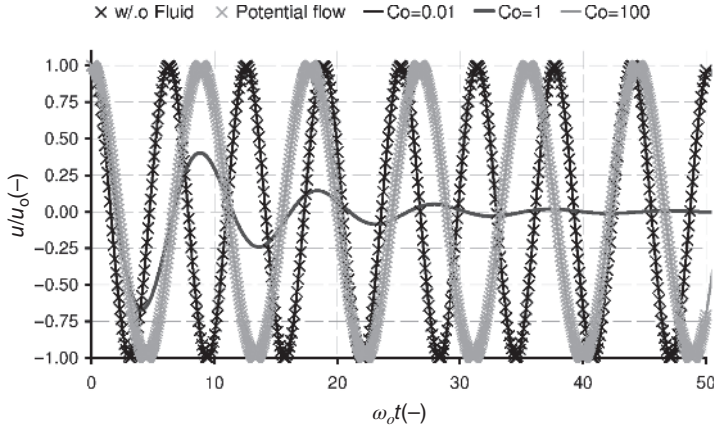
where K is the modified Bessel function of the second kind and the first order (Abramowitz and Stegun, 1970).

The fluid force may thereby be expressed as follows:

$$\hat{\phi}(s) = -\rho \pi R^2 \hat{\mu}(s)\hat{\ddot{u}}(s)$$

Figure 1.10   Cylinder coupled to a compressible fluid in an unbounded domain

Figure 1.11   FSI effects for acoustic flow. The free vibrations of the cylinder without and with fluid are represented using non-dimensional values, for initial conditions $u_o^* = 1$ and $\dot{u}_o^* = 0$ and for various compressibility numbers. For large values of C_o on the one hand, FSI is mainly of inertial nature: the system behaves as if coupled to an incompressible fluid. For small values of C_o on the other hand, FSI may safely be neglected and the system behaves as if no fluid were present. For intermediate values of C_o, FSI combines inertial and radiative effects: some kinetic energy is conveyed by the vibrating cylinder to the fluid, which in turn propagates this energy throughout the external domain. This corresponds to an energy loss for the structure, hence its vibrations are damped

where the FSI function reads as

$$\hat{\mu}(s) = -\frac{1}{Rs/c}\frac{K(Rs/c)}{K'(Rs/c)}$$

The equation of motion of the cylinder in the Laplace domain using non-dimensional variables is then expressed as follows:

$$(1 + \mathcal{M}_a\hat{\mu}(s^*/C_o))\hat{\ddot{u}}^* + \hat{u}^* = 0 \tag{1.4}$$

with:

$$C_o = \frac{c}{\omega_o R}$$

C_o is the so-called *compressibility number*: it may be interpreted as the ratio between the propagation velocity of acoustic waves in the fluid and the vibration velocity of the cylinder.

In the same manner as for the viscous flow, the influence of the fluid on the solid motion is expressed by the FSI function $\hat{\mu}(s^*/C_o)$. The history effect is associated here with the propagation of acoustic waves in the fluid, and it is quantified by the compressibility number[3], as evidenced in Figure 1.11.

Remark 1.1 Radiative damping without inertial effect *In the example depicted in Figure 1.10 and discussed above, FSI is, as a general rule, a combination of inertial effect*

---

[3] It is stressed here that viscous and radiative damping are different in nature, since the latter corresponds to energy dissipation away from the structure by travelling waves, whereas the former corresponds to energy dissipation in the shear layer of the fluid, that is, in the vicinity of the structure.
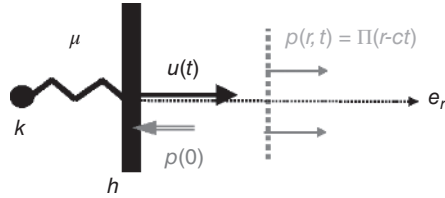
Figure 1.12   *Plate coupled to a compressible fluid in an unbounded domain*

and acoustic damping. In some particular cases however, only a single effect is observed, as evidenced by the following example represented in Figure 1.12.

The motion of the plate is governed by a second-order differential equation:

$$\mu h \ddot{u} + ku = -p|_{r=0}$$

where the pressure field complies with the wave equation, stated here as follows:

$$\frac{1}{c^2}\frac{\partial^2 p}{\partial t^2} - \frac{\partial^2 p}{\partial r^2} = 0$$

and endowed with a non-reflection condition at infinity and a coupling condition with the moving wall at $r = 0$:

$$\left.\frac{\partial p}{\partial r}\right|_{r=0} = -\rho\ddot{u}$$

As detailed in Chapter 3, the pressure field is found to be $p(r,t) = \Pi(r - ct)$: it describes a plane wave propagating away from the moving plate. The coupling condition is $\Pi'(-ct) = -\rho\ddot{u}$ so that the wall pressure is found to be $p|_{r=0} = \Pi(-ct) = \rho c\dot{u}$. The plate motion is thereby
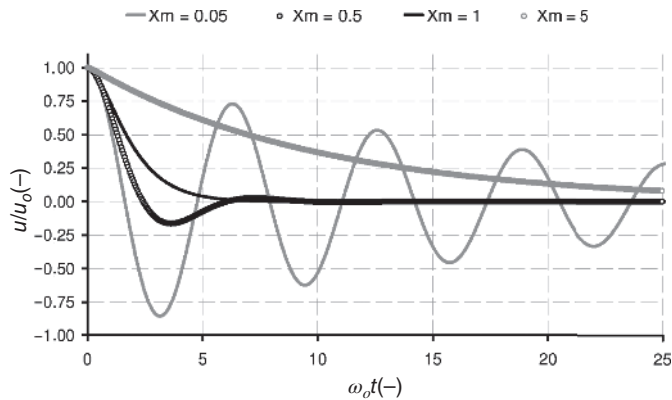
Figure 1.13   **Radiative damping**. *For a plate/plane wave coupled system, FSI is found to be of dissipative nature as a result of radiation. This is visible in the graph which plots the displacement of the system in the time domain with the initial conditions $u(0)/u_o = 1$, $\dot{u}(0)/\dot{u}_o = 0$, and which evidences the typical free oscillation regimes:* (i) *the pseudo-periodic regime* ($\mathcal{X}_m < 1$); (ii) *the aperiodic regime* ($\mathcal{X}_m > 1$); (iii) *the critical aperiodic regime* ($\mathcal{X}_m = 1$)

governed by the differential equation $\mu h\ddot{u} + \rho c\dot{u} + ku = 0$. In a non-dimensional form, the latter equation may be recast as follows:

$$\ddot{u}^* + 2\mathcal{X}_m\dot{u}^* + u^* = 0$$

with $\mathcal{X}_m = \frac{1}{2}\frac{\rho}{\mu}\frac{c}{\omega_o h}$.

As a remarkable feature of FSI in this case, radiative damping solely governs the interaction, which could be counter-intuitive at first glance.[4] $\mathcal{X}_m = 1/2\mathcal{M}_a\mathcal{C}_o$ combines mass number and compressibility number and quantifies radiative damping, as evidenced in Figure 1.13. ■

Further discussions on FSI effects for diversified fluid flow configurations may be found in many textbooks, which provide a deeper insight into the topic: for instance, Axisa (2007) investigates various physical aspects of fluid–structure coupling for stagnant fluids, Païdoussis (2004) and Païdoussis *et al.* (2011) propose an extensive overview of fluid–structure interactions, particularly on stability issues for structures subjected to axial flows or cross-flows.

1.3   Numerical Simulation of Fluid–Structure Interactions

The continuous development of numerical techniques and the constant growth of computational capacities make it possible to perform complex simulations, which account for various multi-physic coupling, among which fluid and structure interactions.

Simulation of FSI tends to become a specific topic in Computational Mechanics, as exposed, for instance, in Bungartz and Schäffer (2006), Benson and Souli (2010), Bazilevs *et al.* (2013) and Bodnar *et al.* (2014), and opens new paths in structural analysis for exploring and evaluating new concepts or designs, especially in applications where the empirical approach is dominant, for instance, in the design of musical instruments (Derveau *et al.*, 2003).

As an illustration of some of the numerical techniques available to the researcher and the practitioner, a few specific examples of FSI simulations are reported in Figure 1.14.

The nature of the physics involved in fluid and structure interactions is so diverse, and the scope of the numerical methods which can be used to represent them is so large that it is difficult to propose a general classification of FSI computational techniques. However, the vast majority of existing methods may be found to belong to one of the approaches depicted in Figure 1.15, the choice of a particular numerical strategy being always a compromise between computational cost, accuracy, robustness and stability.

Using a fluid–structure code is possible when a mathematical model of the coupled problem is established in a form which is suited for numerical discretisation with a unique technique (in terms of space and time discretisations); see for instance Le Tallec and Mouro (2001). This approach is therefore adapted to strong coupling mechanisms and it achieves high accuracy and stability; in terms of modelling and computing, this methodology generally requires a dedicated code to be developed and it proves very costly, especially for non-linear

---

[4] This example is not only worthy of interest from the pedagogic standpoint, but it has also some practical relevance, in particular, for the pre-design of naval or offshore structures (Shin, 2004). The response of a submerged structure to a pressure impulse triggered by a distant underwater explosion may indeed be accounted for with the plate/plane wave interaction model as further discussed by Taylor (1941).

Fluid–structure code

Analytical   Numerical

(a)   (b)

Fluid and structure codes

(c)   (d)
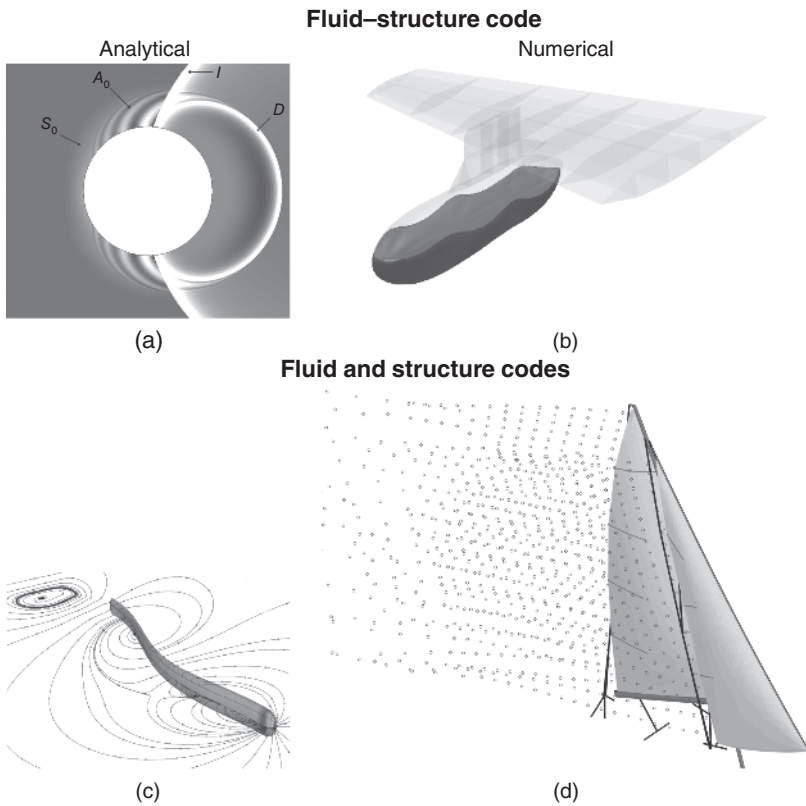
Figure 1.14   Examples of FSI simulations. (a) Leblond *et al.* (2009) develop a coupled model to tackle the vibro-acoustics of submerged shells. The partial differential equations involved in the model are solved in a single code, which allows the description of specific aspects of the interaction. The incoming acoustic wave (I) is diffracted by the shell (D) whose vibrations generate waves in the fluid (A_0 and S_0). The simulation is in good agreement with experimental observations discussed in Ahyi *et al.* (1998). (b) Schotte and Ohayon (2009) formulate a mathematical model accounting for free surface effects in deformable reservoirs of complex shape. The coupled problem is solved using the Finite Element Method (FEM), according to the general principles which will be detailed in Chapter 5. *Source*: Jean-Sébastien SCHOTTÉ, ONREA, Chatillon, France, 2009. Reproduced with permission of Jean-Sébastien SCHOTTÉ. (c) Leroyer and Visonneau (2005) investigate the self-propulsion of a fish-like body, using a numerical procedure which couples the resolution of the Navier–Stokes equation (describing the fluid flow) with a finite volume method (FVM) in Eulerian formulation and the resolution of the Newton law equations (accounting for the structure motion) with a finite element technique in Lagrangian formulation. *Source*: Alban LEROYER, Ecole Centrale, Nantes, France, 2005. Reproduced with permission of Alban LEROYER. (d) Augier *et al.* (2012) propose a numerical model for yacht sail design, by coupling a finite element model composed of beams, cables and membranes, which are standing for the constitutive parts of the boat (*e.g.* spars, rigging and sails), with a vortex lattice method (VLM), which is suited for external fluid flows where vorticity develops in the vicinity of lifting surfaces. *Source*: Patrick BOT, Ecole Navale, Brest, France, 2014. Reproduced with permission of Patrick BOT
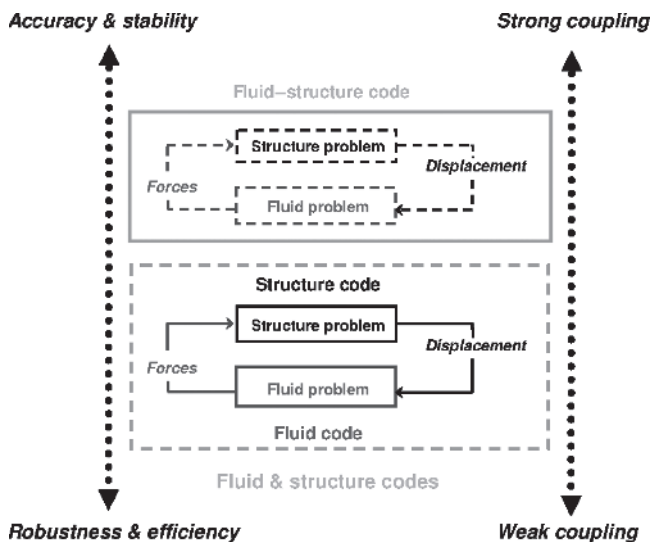
Figure 1.15   Numerical simulation of FSI: coupled fluid–structure code or fluid and structure codes coupling strategy

problems. As exposed in Chapter 5, this strategy is however suited for linear problems formulated on a fixed domain, among which coupled problems involved in vibro-acoustics.

Coupling fluid and structure codes takes advantage of the robustness of each numerical tool and provides efficient solutions for engineering purposes (Felippa *et al.*, 2001; Degroote and Vierendeels, 2011). This *partitioned approach* has widely been investigated since the pioneer researches of Farhat and Piperno (1997) for aero-elastic simulations. Such a methodology requires the development of specific formulations, such as Arbitrary Lagrangian–Eulerian (ALE), and a coupling procedure which allows for space and time coupling (Casadeï *et al.*, 2001).

- ALE (Donea *et al.*, 1982) is particularly suited to simulate FSI, since it combines the Lagrangian formulation, which is the standard framework for structural dynamics, and the Eulerian formulation, which is adapted to fluid dynamics; see Figure 1.16.

  With the Eulerian formulation, the equation of motion is written in a spatial domain so that the system moves through a fixed grid: this approach is therefore particularly suited to the description of fluid flows. In the Lagrangian formulation, the equation of motion is written in a material domain: the motion is tracked by a grid which deforms while the system moves. This approach is adapted for structures undergoing large displacements, as long as the grid deformation remains limited.

  Arbitrary Lagrangian–Eulerian formulation combines both descriptions by stating the equation of motion in a moving frame: it allows a control of the mesh geometry independently from the material geometry. ALE is of broad use and interest in the context of FSI simulation, since large deformations of the fluid–structure interface can be conveniently
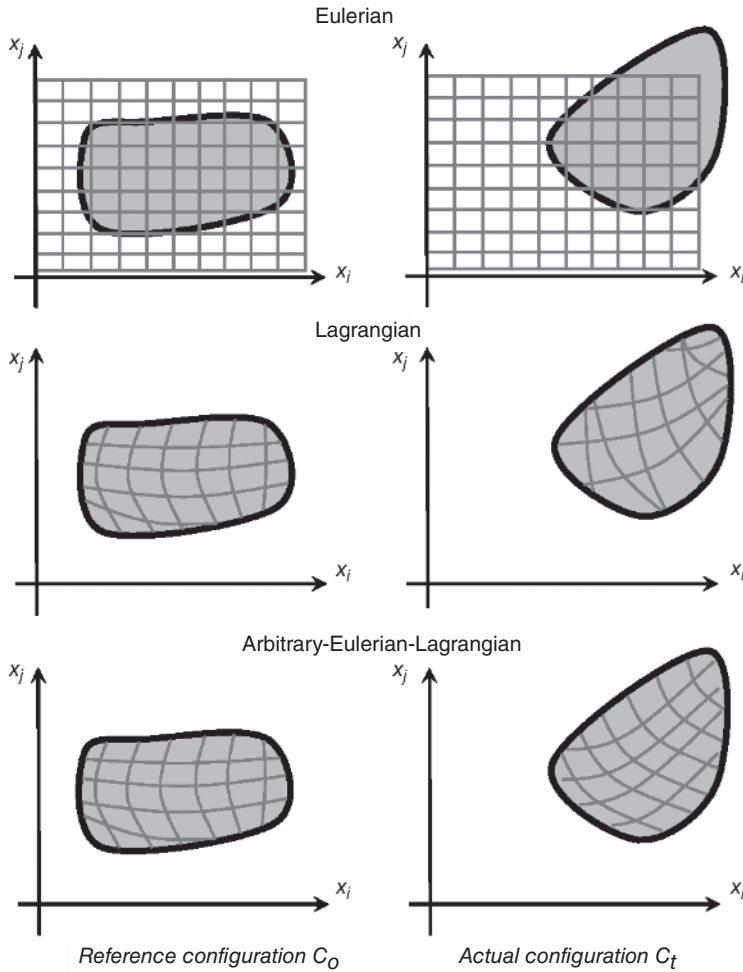
Figure 1.16   Lagrangian, Eulerian and Arbitrary Lagrangian–Eulerian formulations

handled – with a Lagrangian-dominated approach to adjust the structure motion, while the physics of the fluid flow is accounted for with an Eulerian-dominated approach (Souli *et al.*, 2000).

For small transformations about an equilibrium state, which is the framework adopted in this book to describe the vibrations of a structure or a fluid (as discussed further in Chapters 2 and 3), the Lagrangian and Eulerian formulations are equivalent.

- Coupling in space handles the information exchanges between the two codes involved in the simulation (Farhat *et al.*, 1998). The first one, referred to as the *CSD code*[5] solves the equation of motion of the structure subsystem, while the second one, referred to as the

---

[5] As discussed in Chapter 6, CSD stands for *Computational Structural Dynamics* and designates the set of numerical techniques available to solve the second-order ordinary differential equations which account for the motion of mechanical systems.
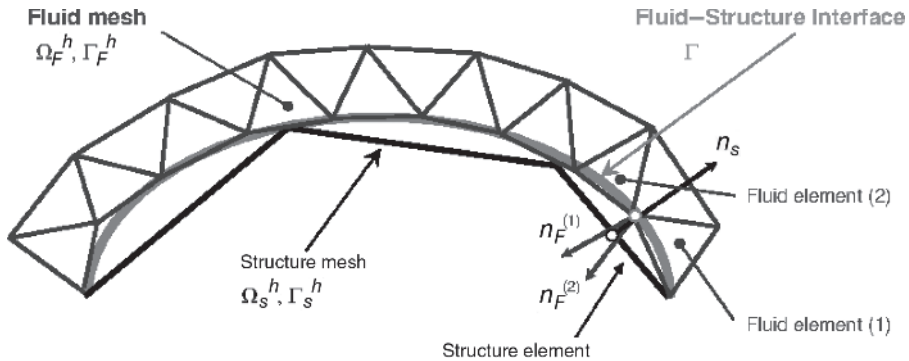
Figure 1.17   Space coupling. The finite volume method (FVM) and the finite element method (FEM) are typically used as discretisation techniques, respectively, for Computational Fluid Dynamics (CFD) and Computational Structural Dynamics (CSD). As different physics are represented by each code, different meshes may be required to solve the equations of each sub-problems: at the fluid–structure interface, where force and motion are transferred from one code to another, the compatibility between the fluid and structure meshes is not always possible. Consequently, the definition of the normal at the interface may be ambiguous, as depicted above. Various techniques may be used to convert the pressure computed on one node in the fluid mesh to the corresponding finite element in the structure mesh, for instance with interpolation finite elements (Guruswamy, 1989). As an approximation of the exchanges is inevitably introduced by the discretisation of the interface, the projection technique should be designed in order to limit energy losses (Piperno and Farhat, 2001)

    CFD code,[6] each of the two codes may make use of different discretisation and approximation techniques.

    The space coupling is therefore designed to be as accurate as possible in order to limit the loss of information, hence of energy, due to discretisation and approximation (Maman and Farhat, 1995; Piperno and Farhat, 2001), see for instance Figure 1.17.

- Coupling in time organises the information exchanges between two time iterations of the codes and achieves a strong or weak coupling: as a delay is introduced between the structure and fluid codes, some energy is lost between iterations. Inaccuracies and instabilities in the simulation may result from the use of algorithms which would fail to correctly account for the mechanical coupling (Piperno *et al.*, 1995), see for instance Figure 1.18.

    From a practical point of view, CFD–CSD numerical strategies are relatively mature for many industrial applications; they are commonly based on general procedures, such as the one described in Figure 1.19: coupling techniques are accessible to the engineer with a combination of various CFD and CSD codes; see for instance Gaugain (2013) and Yvin (2014).

    The architecture of code coupling depends on the problem under concern, whether FSI is driven by the fluid flow or by the structural response. Robust simulations are often based on staggered or iterated procedures: within a time loop, a coupling loop handles the exchanges between the two codes. The fluid force is passed from the CFD code to the CSD code and, conversely, the fluid–structure interface motion from the CSD code to the CFD code. When large

---

[6] CFD stands for *Computational Fluid Dynamics* and, as illustrated in Remark 3.1, it refers to the numerical techniques aimed at solving the equations of fluid flows.
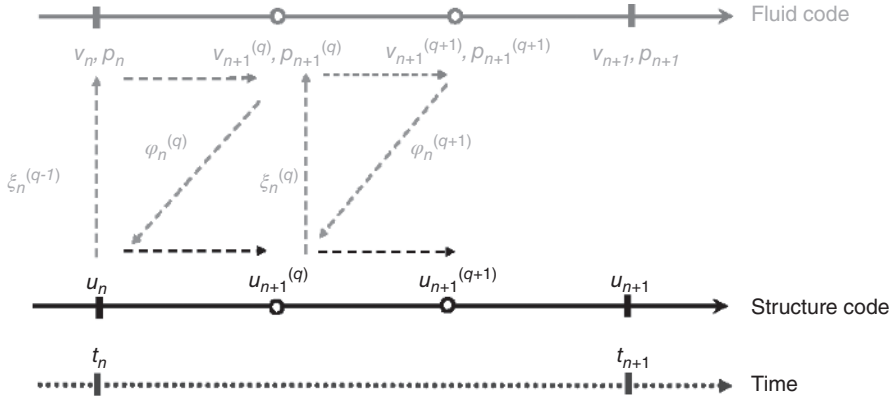
Figure 1.18 Time coupling. From time t_n to time t_{n+1}, CFD and CSD codes are coupled in a staggered manner: the structure displacement $\mathbf{u}_n$ and the fluid–structure interface motion $\boldsymbol{\xi}_n$ are first computed and serve as boundary conditions for the CFD code. The latter computes the fluid pressure and velocity fields p_n and $\mathbf{v}_n$, yielding the fluid force on the structure $\boldsymbol{\varphi}_n$. The CSD code computes the displacement which results from the loading on the structure. Iterations of this procedure within a time step $[t_n, t_{n+1}]$ produce a sequence of structure and pressure fields $\mathbf{u}_n^q, \boldsymbol{\xi}_n^q, p_n^q, \mathbf{v}_n^q$ and $\boldsymbol{\varphi}_n^q$. It gives the updated fields at time t_{n+1} when a convergence criterion is satisfied (Schäffer and Teschauer, 2001)

displacements of the structure are accounted for, the mesh of the fluid problem is modified: this is usually achieved with moving mesh and/or re-meshing techniques; see for instance Figure 1.20.

Iteration of the process is required when the fluid and the structure are 'strongly' coupled. Achieving accuracy and stability demands an important computational effort: coupled strategies based on ALE formulation are in general not affordable for 'highly non-linear' problems.

Although coupled simulations achieve satisfying levels of accuracy and reliability for industrial and academic purposes, it should be mentioned that for the sake of robustness, multi-physic algorithms offered by general-purpose codes are often adapted from coupling strategies presented in the scientific literature: a theoretical and practical involvement is therefore required from any code user to validate the coupling procedures.

Experimental tests on academic cases provide fruitful data for code verification, together with physical insights which guide numerical simulations, as illustrated for instance in Figures 1.21 and 1.22. Experiments and numerics often proceed in a joined manner: on the one hand, a mathematical model is an ideal representation of the physical world, so that a numerical method always exhibits finite accuracy; on the other hand, the reproducibility of experiments is often questionable and data acquisition is always limited. A meaningful numerical/experimental validation might stem from crossing error estimates in simulations with uncertainty quantification in experiments.

When experimental data are not available, it may be worthy of interest to turn to analytical solutions. As outlined in the previous section, analytical models generally deal with simple geometry and physics, but provide some deeper insights into a particular aspect and may serve as a reference for validation purposes; see for instance (Placzek *et al.*, 2009).
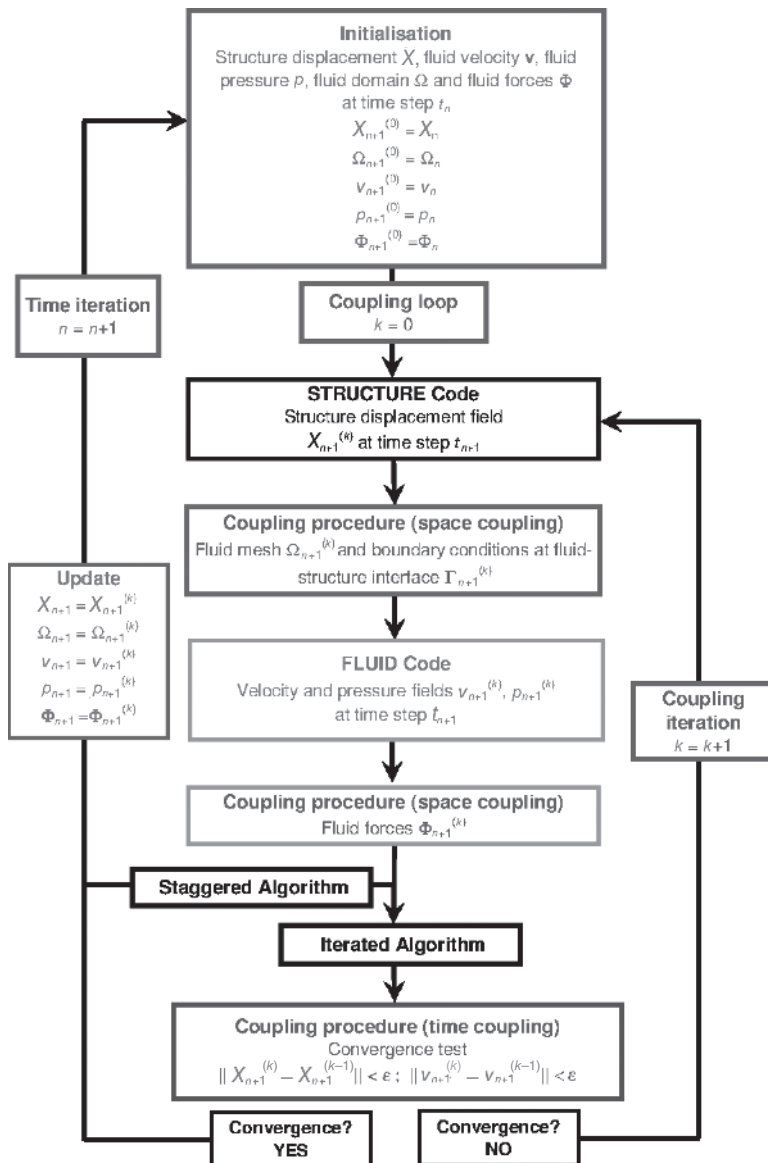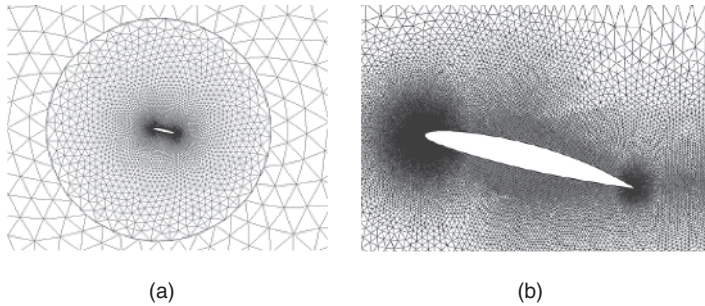
Figure 1.19   Simulation of FSI with CSD and CFD coupling

<div align="center">(a)   (b)</div>

Figure 1.20   Moving mesh technique. The moving mesh techniques – for instance with sliding mesh (a) or deforming mesh (b) – are well suited to FSI simulation since they allow for the mesh to adjust to the motion of boundaries, as is the case in the present example, which is concerned with the pitching motion of a hydrofoil in a fluid flow (Ducoin *et al.*, 2009)

1.4   Finite Element and Boundary Element Methods

As suggested by the earlier examples, FSI may be addressed from various points of view, whether the fluid is confined in the structure or contains the structure, whether the fluid is stagnant or flowing. In this case, an additional complexity arises from the flow conditions, which may be compressible or incompressible, separated or attached, laminar or turbulent.

Among the many techniques which are available to the practitioner, Figure 1.23 gives a simplified overview of coupling methods which are of common use for engineering purposes.

Flow–Structure Interaction is generally described with *time-domain equations* in the *actual configuration* of the system: coupling CSD and CFD codes, as presented in the previous section, is, among various options, one of the most convenient strategies to tackle FSI.

Fluid–Structure Interaction is usually modelled with equations of motion written in the *frequency domain* (for linear problems, it is equivalent to a time-domain formulation, through the Laplace transform). Since small displacements of the fluid and structure are considered, these equations are stated in the *reference configuration* of the system. Coupling fluid and structure finite elements is adapted to problems involving a fluid contained in a structure. *Infinite elements* or *boundary elements* allows for FSI modelling when considering structures submerged in an unbounded fluid domain. In the former case, a unique finite element code solves the coupled problem, whereas in the latter two codes may need to be coupled.

This book is centred for the most part on the mathematical modelling and on the numerical simulation of FSI, for elastic *structures* coupled to a *quiescent* fluid, whether bounded or not, using *finite element* or *boundary element* methods. According to the FEM, both the continuous domain and its boundaries are discretised, while according to the Boundary Element Method (BEM), the discretisation is restricted to the boundaries, which may be advantageous in terms of computational effort when one has to deal with a large, or even infinite, extent of fluid – in the latter case, the unbounded character of the fluid domain may also be tackled with the infinite element method (IEM).
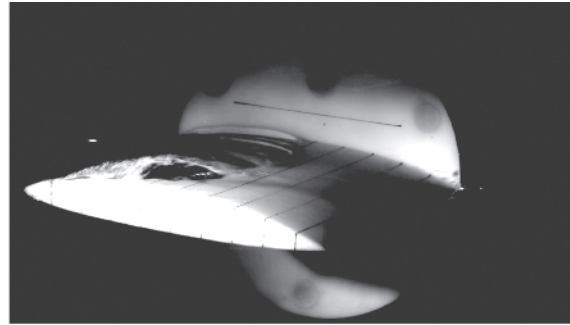
(a)
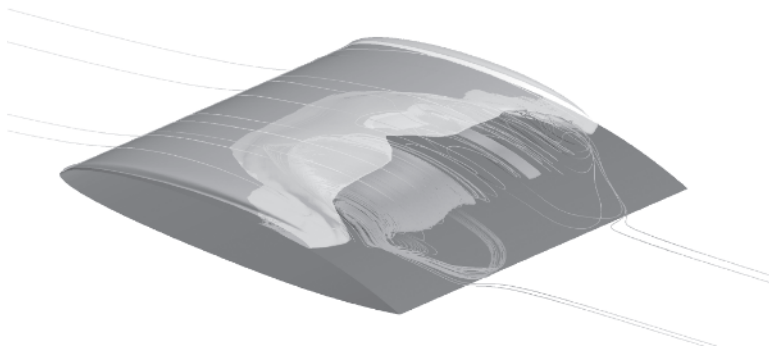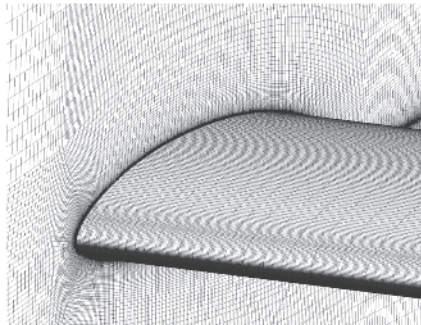
(b)

Figure 1.21   Hydrodynamics and Fluid–Structure Interaction. (a) Experiments provide meaningful data to understand the physics of complex interactions, such as the one evidenced in Ducoin *et al.* (2012) as far as the dynamic behaviour of an elastic hydrofoil in cavitating flow is concerned. (b) Coupling between the formation of sheet cavitation and the vibrations of the hydrofoil is accurately reproduced with CFD–CSD coupling procedures built with general-purpose numerical codes (Gaugain *et al.*, 2012). *Source*: André Astolfi, Ecole Navale, Brest, France and Fabien Gaugain, DCNS Research, Nantes, France, 2013. Reproduced with permission of André Astolfi
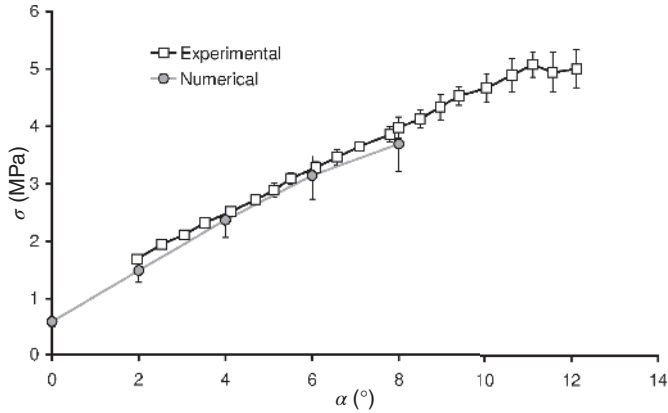
(a)
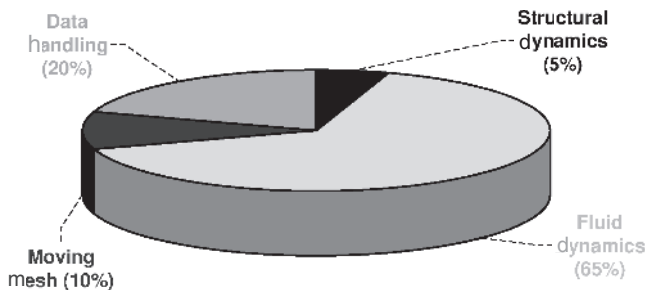
(b)

Figure 1.22   Hydrodynamics and Fluid–Structure Interaction (continued). (a) In the example proposed in (Gaugain, 2013), the agreement between experiments and simulations is quite remarkable and builds confidence in the future engineering applications of the numerical tool. (b) For such simulations, the computational cost is mostly driven by CFD, but moving mesh and data handling are also demanding. However, coupled simulations which capture some fine physics remain today out of reach for large industrial applications

The vibrations of structure and fluid systems, as well as the finite element method and the boundary element method, are introduced in Chapters 2 and 3. Finite element coupling is then described in Chapter 4 for the modelling of inertial effects. Fluid–structure coupling is addressed in Chapter 5, mainly focussing on vibro-acoustics; various mathematical formulations of the coupled problem are detailed and discussed. Structural dynamics with FSI, either for time-domain or for frequency-domain analyses, is finally presented in Chapter 6. Numerous application examples are also proposed to deepen the analysis; each of them has been programmed using MATLAB, which offers a convenient approach of numerical methods for engineers (Kiusalaas, 2005).
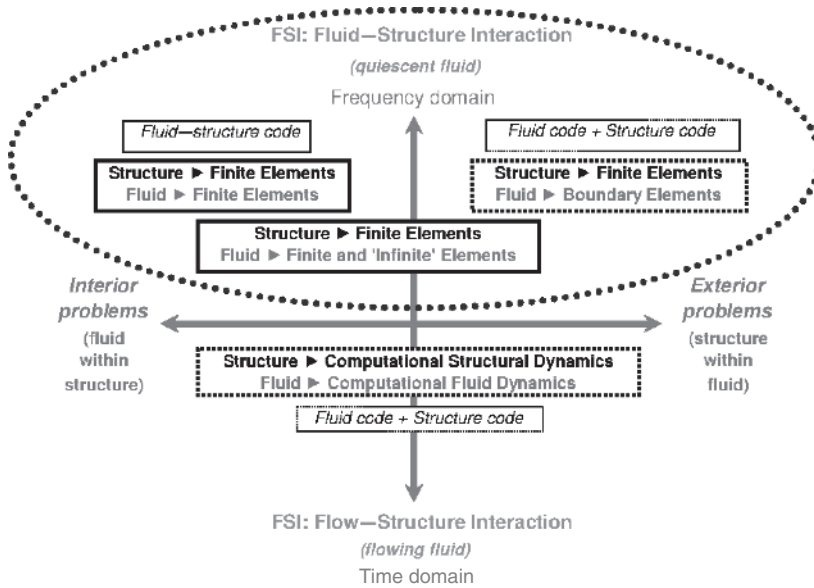
Figure 1.23   Engineering methods for FSI simulations

References

Abramowitz M and Stegun IA 1970 *Handbook of Mathematical Functions*. Dover Publications.

Ahyi AC, Pernod P, Gatti O, Lattard V, Merlen A, and Uberall H 1998 Experimental demonstration of the pseudo-Rayleigh wave. *Journal of Acoustical Society of America*, **104**, 2727–2732.

Augier B, Bot P, Auville F, and Durand M 2012 Dynamic behaviour of a flexible yatch sail plan. *Ocean Engineering*, **66**, 32–43.

Axisa F 2007 *Modelling of Mechanical Systems – Fluid-Structure Interaction*. Elsevier.

Bazilevs Y, Takizawa K, and Tezduyar TE 2013 *Computational Fluid-Structure Interaction: Methods and Applications*. John Wiley & Sons, Ltd.

Benson DJ and Souli M 2010 *Arbitrary Lagrangian Eulerian and Fluid-Structure Interaction: Numerical Simulation*. John Wiley & Sons, Ltd.

Bodnar T, Galdi GP, and Necasova S 2014 *Fluid-Structure Interaction and Biomedical Applications*. Springer-Verlag.

Bundgartz J and Schäffer M 2006 *Fluid-Structure Interaction: Modelling, Simulation, Optimization*. Springer-Verlag.

Casadëi F, alleux JP, Sala A, and Chille F. 2001 Transient fluid-structure interaction algorithms for large industrial applications. *Computer Methods in Applied Mechanics and Engineering*, **190**, 3081–3110.

Degroote J and Vierendeels J 2011 Multi-solver algorithms for the partitioned simulation of fluid-structure interaction. *Computer Methods in Applied Mechanics and Engineering*, **200**, 2195–2210.

De Langre E 2001 *Fluides et solides*. Editions de l'Ecole Polytechnique.

Derveau G, Chaigne A, Joly P, and Béchade E 2003 Time-domain simulation of a guitar: model and method. *Journal of the Acoustical Society of America*, **114**, 3368–3383.

Donea J, Guiliani S, and Halleux JP 1982 An Arbitrary-Lagrangian-Eulerian finite element method for transient dynamic fluid-structure interaction. *Computer Methods in Applied Mechanics and Engineering*, **33**, 689–723.

Ducoin A, Astolfi JA, Deniset F, and Sigrist JF 2009 Computational and experimental investigation of flow over a transient pitching hydrofoil. *European Journal of Mechanics - B/Fluids*, **28**, 728–743.

Ducoin A, Astolfi JA, and Sigrist JF 2012 An Experimental analysis of fluid-structure interaction on a flexible hydro-foil in various flow regimes including cavitating flow. *European Journal of Mechanics - B/Fluids*, **36**, 63–74.

Farhat C, Lesoinne M, and Le Tallec P 1998 Load and motion transfer algorithm for fluid-structure interaction problems with non-matching discrete interfaces: momentum and energy conservation, optimal discretisation and application to aeroelasticity. *Computer Methods in Applied Mechanics and Engineering*, **157**, 95–114.

Felippa C, Park KC, and Farhat C 2001 Partitioned analysis of coupled mechanical systems. *Computer Methods in Applied Mechanics and Engineering*, **190**, 3247–3270.

Fritz RJ 1972 The Effect of liquids on the dynamic motion of immersed solids. *Journal of Engineering for Industry*, **91**, 167–173.

Gaugain F 2013 Analyse expérimentale et simulations numériques de l'interaction fluide-structure d'un hydrofoild élastique en écoulement cavitant et subcavitant. PhD thesis, Ecole Nationale Supérieure des Arts & Métiers, Paris.

Gaugain F, Astolfi A, Sigrist JF, and Deniset F 2012 Numerical and experimental study of the hydroelastic behaviour of an hydrofoil. In *Proceedings of the 10th International Conference on Flow Induced Vibration (FIV 2012)*.

Guruswamy GP 1989 Integrated approach for active coupling of structures and fluid. *AIAA Journal*, **27**, 788–793.

Kiusalaas J 2005 *Numerical Methods in Engineering with MATLAB*. Cambridge University Press.

Leblond C, Iakovlev S, and Sigrist JF 2009. A fully elastic model for studying submerged circular cylindrical shells subjected to a weak shock wave. *Mécanique & Industries*, **10**, 275–284.

Leblond C, Sigrist JF, Auvity B, and Peerhossaini H 2009 A Semi-analytical approach for the study of an elastic circular cylinder in cylindrical fluid domain subjected to small amplitude transient motion. *Journal of Fluids and Structures*, **25**, 134–154.

Leroyer A and Visonneau M 2005 Numerical methods for RANSE simulations of a self-propelled fish-like body. *Journal of Fluids and Structures*, **20**, 975–991.

Le Tallec P and Mouro J 2001 Fluid-structure interaction with large structural displacements. *Computer Methods in Applied Mechanics and Engineering*, **190**, 3039–3067.

Maman N and Farhat C 1995 Matching fluid and structure meshes for aeroelastic computations: a parallel approach. *Computers & Structures*, **54**, 779–785.

Païdoussis MP 2004 *Fluid-Structure Interactions: Slender Structures and Axial Flow*. Academic Press.

Païdoussis MP, Price SJ, and De Langre E 2011 *Fluid-Structure Interactions – Cross-Flow-Induced Instabilities*. Cambridge University Press.

Piperno S 1997 Explicit-implicit fluid-structure staggered procedures with a structural predictor and fluid subcycling for 2D inviscid aeroelastic simulations. *International Journal for Numerical Methods in Fluids*, **25**, 1207–1226.

Piperno S and Farhat C 2001 Partitioned procedures for the transient solution of coupled aeroelastic problems. Part II: energy transfer analysis and three-dimensional application. *Computer Methods in Applied Mechanics and Engineering*, **190**, 3147–3170.

Piperno S, Farhat C, and Larrouturou B 1995 Partitioned procedures for the transient solution of coupled aeroelastic problems. Part I: model problem, theory and two-dimensional application. *Computer Methods in Applied Mechanical and Engineering*, **124**, 79–112.

Placzek A, Sigrist JF, and Hamdouni A 2009 Numerical simulation of an oscillating cylinder in a cross-flow at low Reynolds number: forced and free oscillations. *Computers & Fluids*, **38**, 80–100.

Schäffer M and Teschauer I 2001 Numerical simulation of coupled fluid-solid problems. *Computer Methods in Applied Mechanics and Engineering*, **190**, 3645–3667.

Schotté JS and Ohayon R 2009 Various modelling levels to represent internal liquid behaviour in the vibratory analysis of complex structures. *Computer Methods in Applied Mechanics and Engineering*, **198**, 1913–1925.

Shin Y 2004 Ship shock modelling and simulation of far-field underwater explosion. *Computers and Structures*, **82**, 2211–2219.

Souli M, Ouahsine A, and Lewin L 2000 ALE formulation for fluid-structure interaction problems. *Computer Methods in Applied Mechanics and Engineering*, **190**, 659–675.

Taylor GI 1941 *The Pressure and Impulse of Submarine Explosion Waves on Plate*. Cambridge University Press.

Yvin C 2014. Interaction fluide-structure pour des configurations multi-corps. Applications aux liaisons complexes, lois de commande d'actionneur et systèmes souples dans le domaine maritime. PhD thesis, Ecole Centrale, Nantes.